Carbohydrate Polymer Technologies and Applications 10 (2025) 100766

Contents lists available at ScienceDirect

Carbohydrate Polymer Technologies and Applications

journal homepage: www.sciencedirect.com/journal/carbohydrate-polymer-technologies-and-applications

Preparation and characterization of alginate-based capsules containing lavender essential oil for acne therapy

Yasmin Kabalan [a], Héloïse Bernarda [a], Xavier Montané [b,*], Silvia De la Flor [c], Bartosz Tylkowski [a,d], Anna Trojanowska [a], Annalisa La Gatta [e], Marta Giamberini [a,*]

[a] Department of Chemical Engineering, Universitat Rovira i Virgili, Av. Països Catalans 26, 43007 Tarragona, Spain
[b] Department of Analytical Chemistry and Organic Chemistry, Universitat Rovira i Virgili, C/Marcel·lí Domingo 1, 43007 Tarragona, Spain
[c] Department of Mechanical Engineering, Universitat Rovira i Virgili, Av. Països Catalans 26, 43007 Tarragona, Spain
[d] Eurecat, Centre Tecnològic de Catalunya, Unitat de Tecnologia Química, C/ Marcel·lí Domingo 2, 43007 Tarragona, Spain
[e] Department of Experimental Medicine, Section of Biotechnology, Medical Histology and Molecular Biology, University of Campania "Luigi Vanvitelli", via L. De Crecchio 7, 80138 Naples, Italy

ARTICLE INFO

Keywords:
Alginate capsule
Lavender oil
Nanoemulsion
Ionic gelation
Acne treatment

ABSTRACT

In this study, we prepared alginate-based capsules containing lavender essential oil for cosmetic applications and acne treatment. To tune their preparation, several parameters have been changed to obtain empty and oil-containing beads, i.e. the alginate molecular weight and concentration and the cation concentration. Calcium-crosslinked beads were also studied as a reference system. The capsules were characterized by Optical Microscopy (OM), Environmental Scanning Electron Microscopy (ESEM), Thermogravimetric Analysis (TGA) and Dynamic Mechanical Analysis (DMA), while Encapsulation Efficiency was calculated by Gas Chromatography-Mass Spectrometry (GC–MS). Significant differences in the morphology of empty capsules are observed depending on the concentration of cation used and of the alginate solution; differently, capsules containing oil, regardless of the cation used, have a smooth surface and a highly porous interior. Encapsulation efficiency was very good, averaging 98 % for all samples. As for the mechanical properties of the capsules, the Young Modulus and the force at break were determined for oily and empty capsules with both cations. The empty capsules resulted more rigid and resistant than the oil-containing ones, while the latter showed an elastoplastic behaviour.

1. Introduction

In recent years, the field of cosmetics and dermatology has proven its importance in our daily lives where the global revenue is estimated to continuously increase between 2024 and 2029 by 22.04 % (Revenue of the cosmetics industry worldwide 2019–2029, 2024). Nowadays, many cosmetics and personal care products contain biologically active molecules that require encapsulation for their protection and increased stability (Chu et al., 2021); additionally, the delivery of active cosmetic compounds requires effective, controlled, and safe means of reaching the target site within the skin Santos et al. (2019). Encapsulation has proven as an efficient and practical way to meet all these specifications (Siqueira Andrade et al., 2024). The encapsulated agent can be then released by several mechanisms, such as mechanical action and heat that are adequate when applying a cosmetic product (Casanova & Santos, 2016) .

Acne is a skin disorder which affects around 9.4 % of the people worldwide (Tan & Bhate, 2015), which can occur in people of any age. Indeed, over 20 % of adults in their 30 s report having acne (Collier et al., 2008). It is a chronic inflammatory skin disease that includes pimples, blackheads, and whiteheads, which can appear on the face, back, and chest, acne vulgaris being the most common (Vasam et al., 2023). The increase of androgens' production during puberty determines a sebum excess which, along with dead skin cells, clogs hair follicles which can form blackheads and whiteheads; their eventual inflammation provokes the formation of papules, postules, nodules, or cysts under the skin Ramli et al. (2012). Acne can also be related to hormonal, genetic, dietary and personal factors.

Topical and oral antibiotics, like minocycline and doxycycline, have long been used to treat acne (Del Rosso & Kim, 2009); however, due to the rise in antimicrobial resistance, alternative therapies are now needed (Monteiro & Fernandes, 2024; Walsh et al., 2016). On the other hand,

* Corresponding authors.
E-mail addresses: xavier.montane@urv.cat (X. Montané), marta.giamberini@urv.cat (M. Giamberini).

https://doi.org/10.1016/j.carpta.2025.100766

Available online 17 March 2025

products based on natural raw materials are highly appreciated by consumers: therefore, the use of essential oils (EO) is an increasingly explored option. In fact, several studies showed that EO present antioxidant, antibacterial, and anti-inflammatory effects due to their different phytochemical constituents and active compounds (Asnaashari et al., 2023). In particular, lavender oil (LO) has shown good antibacterial activity against acne related bacteria (Altun et al., 2023). However, due to the volatility of LO and the risks of applying it pure on the skin, encapsulation is the best option for delivering the oil in dermatological products to enhance efficacy (Cimino et al., 2021). Previous studies attempted to encapsulate LO: For example, Sangsuwan et al. prepared alginate and chitosan beads containing LO, but the encapsulation efficiency (EE) did not exceed 20 % (Sangsuwan & Sutthasupa, 2019); Zhang et al. could increase the EE of LO up to 80 %: nevertheless, they achieved this result by synthesizing double layered microcapsules using β-cyclodextrin, alginate and chitosan as wall materials (Zhang et al., 2020).

Alginate biopolymer has recently shown great interest in encapsulation is. Extracted from brown algae, alginate is a natural linear polysaccharide composed of (1–4) linked residues of alpha-l-guluronate (G) and beta-d-mannuronate (M) (Wani et al., 2023). Alginate properties can vary according to the proportion and the sequential arrangements of M or G residues as homo-blocks or hetero-blocks (Sosnik, 2014). Due to its biodegradability and biocompatibility, it is increasingly used in fields like cosmetics and medicine (Ren et al., 2024; Selvasudha et al., 2023). Alginate solutions can form capsules by crosslinking with divalent cations (Dhamecha et al., 2019), which can penetrate the capsules and be trapped in an electronegative cavity formed by the alginate chains. Calcium is often used as a cross-linking agent and recognized as a cation offering interesting properties to alginate beads. However, in this study, we aim at using zinc, an element known for its action against acne. In fact, this element naturally present in our body has antibacterial and anti-inflammatory effects and may reduce sebum secretion (Prasad et al., 2009). Moreover, reduced zinc levels in the body can lead to serious health problems (Ali et al., 2024). People with acne vulgaris often have lower levels of zinc, so oral supplementation may help reduce inflammatory episodes (Searle et al., 2022). However, studies suggest that oral zinc can cause nausea or vomiting, making topical zinc a better option, as it can penetrate the skin to reach the dermis and bloodstream (Rostan et al., 2002; Cervantes et al., 2018). Therefore, using zinc as a cross-linker for alginate could represent a good alternative, possibly having a synergistic effect with LO.

The objective of this study is therefore to encapsulate LO in alginate-based capsules using zinc as a crosslinking agent through combining nanoemulsion and ionic gelation techniques. The study aims at achieving high EE while using minimal material and a simple method. The molecular weight and the M/G ratio of different alginates were assessed to check their influence on the capsules' properties. Alginate capsules, with and without LO oil, were prepared at varying concentrations and with either calcium or zinc to study their influence on the obtained beads; they were then analyzed for EE, morphological, mechanical, and thermal properties. In a forthcoming paper, their antibacterial properties will be examined for potential use in acne therapy.

2. Materials and methods

2.1. Materials

Three batches of sodium alginate were used: the first one, referred as "A" (viscosity (1 % in water; 20 °C): 350–550 mPa-s; MW: 10,000–600,000 g/mol) was purchased from Panreac ITW Reagents. The second one, referred as "B", CEROGA sodium alginate Type NA4012 (viscosity (1 % in water; 20 °C): min 400 mPa.s) was purchased from Roeper GmbH. The third one, referred as "C (viscosity (1 % in water; 25 °C): 5.0–40.0 mPa-s; M_w: 12,000–40,000 g/mol) was purchased from Sigma-Aldrich. $ZnCl_2$ (≥ 98 %) and Mowiol 18–88: Poli(vinil alcohol) (M_w: 130,000 Da, viscosity (1 % in water; 20 °C): 16–20 mPa.s) were purchased from Sigma-Aldrich. $CaCl_2$ (96 %) was purchased from Fisher Scientific. LO (Lavande Maillette) was purchased from Isope Provence. All the chemical compounds were used as provided without any further purification.

2.2. Preparation of the empty capsules

To synthesize the empty capsules, the alginate solution was water diluted (1:5 wt ratio water: alginate solution) to ensure the same final alginate concentration as in the oil capsules. Then 60 g of the prepared solution was extruded using a peristaltic pump (KDS 100 Legacy Syringe Pump, KDScientific) with 1 mL/min flowrate, in the form of drops over a crosslinking bath whose composition and concentration varied according to the different formulations (Table 1). The distance between the needle and the crosslinking bath was fixed at 5.5 cm. Beads immediately formed; during the maturation phase, the capsules were stirred in the crosslinking bath for 48 h, allowing divalent cations to penetrate and crosslink the alginate chains. Gel formation occurred from the outside to the inside of the capsules. Finally, the capsules were filtered, washed twice with distilled water, and left to dry at room temperature for 6 days. They were then stored in glass vials at room temperature.

2.3. Preparation of the oil capsules

To encapsulate LO inside the capsules, a nanoemulsion must first be formed, as the oil is hydrophobic, and the capsules are prepared in an aqueous medium. So, a mixture of 1:5 wt ratio of LO: alginate solution with 0.1 % w/w Mowiol 18–88, as an emulsion stabilizer, was prepared. This mixture was homogenised using a high-speed homogenizer (T25 digital Ultra Turrax, IKA,) at 8000 rpm speed for 30 min. Once the emulsion was prepared, 60 g of the solution were extruded into drops under the same conditions as before. The capsules were left to mature before being collected. After drying, they were stored in glass vials at 4 °C and sealed with parafilm. The overall procedure for the synthesis of the empty and the oil containing capsules is shown in Fig. 1 and the composition of the different batches of the capsules is reported in Table 1.

2.4. Characterization techniques

2.4.1. ^1H nuclear magnetic resonance (NMR)

The ^1H NMR spectra of the three alginate solutions in D_2O were recorded on the spectrometer Varian Gemini 400 MHz (^1H Proton Larmor frequency of – 400 MHz, Bruker Corporation, Billerica, MA, USA) at a temperature of 70 °C, to decrease the alginate viscosity and improve the spectral resolution, with a pulse delay time of 5s. Presaturation was applied during the relaxation delay and mixing time with 25 Hz to remove the water peak from the spectrum, which would have overlapped with one of the alginate peak. The number of scans was 64. For the preparation of the NMR tubes, 20 mg of sodium alginate were dissolved in 1 ml of D_2O.

The software MestReNova (version 6.0.2–5475, Mestrelab Research S.L.) was used for the data analysis and peaks deconvolution.

2.4.2. Size exclusion chromatography-triple detector array (SEC-TDA)

Samples hydrodynamic characterization was carried out using the Size Exclusion Chromatography-Triple Detector Array (SEC-TDA) equipment by Viscotek (Malvern Instruments TDA 305) as described in Gatta et al. (2010).

For each alginate sample (A, B and C), solutions at two diverse concentrations were prepared in double distilled-water and each solution was prepared in triplicate. Samples were then filtered on 0.22 μm and properly diluted for the chromatographic analysis. The latter was carried out as reported in the literature (Gatta et al., 2010), using a dn/dc value equal to 0.157 measured, for the tested samples, within this

Table 1
Composition of the different capsules prepared.

Sample	Alginate used	Alginate Concentration (% w/w)	Crosslinking solution	Crosslinker Concentration (% w/w)	LO/Alginate (% w)
A1-Zn0.5	A	1	$ZnCl_2$	0.5	0
B1-Zn0.5	B	1	$ZnCl_2$	0.5	0
A1-Zn2	A	1	$ZnCl_2$	2	0
A1-Zn2-O	A	1	$ZnCl_2$	2	20
B1-Zn2	B	1	$ZnCl_2$	2	0
B1-Zn2-O	B	1	$ZnCl_2$	2	20
A2-Zn2	A	2	$ZnCl_2$	2	0
A2-Zn2-O	A	2	$ZnCl_2$	2	20
A2-Ca2	A	2	$CaCl_2$	2	0
A2-Ca2-O	A	2	$CaCl_2$	2	20
C1-Ca2	C	1	$CaCl_2$	2	0
C2-Ca2	C	2	$CaCl_2$	2	0

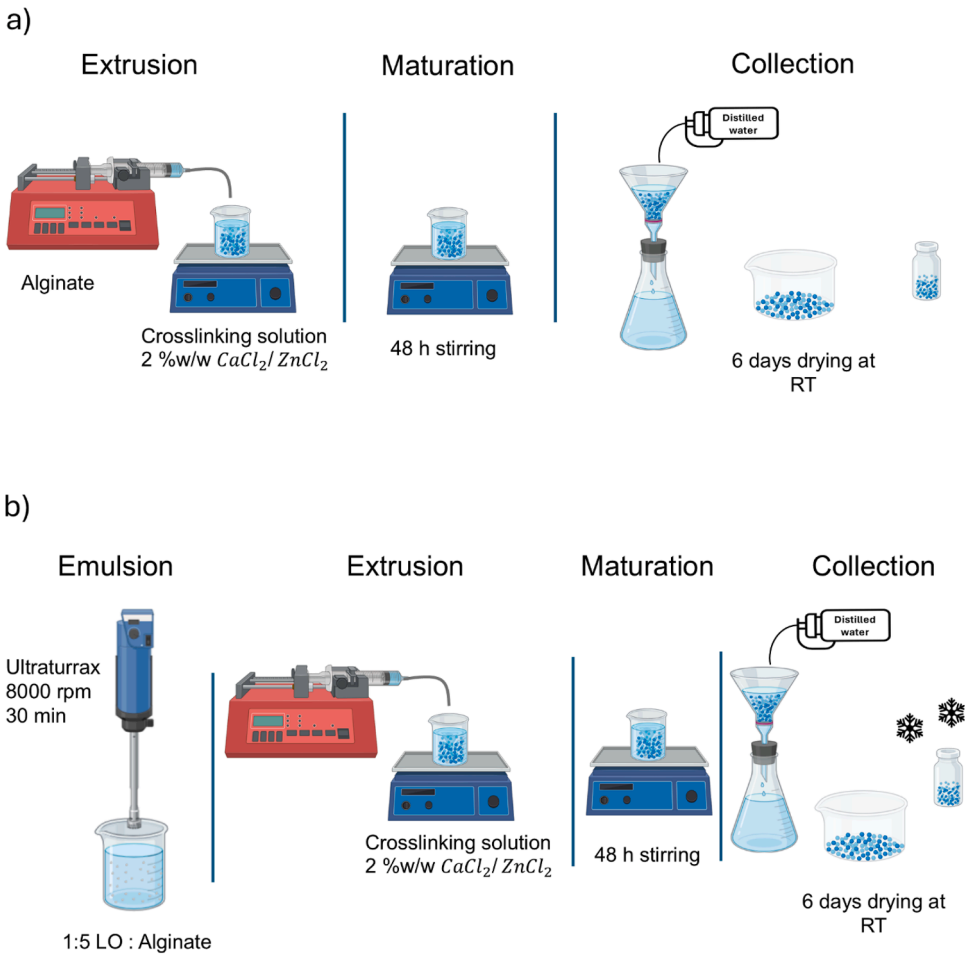

Fig. 1. Preparation procedure of the a) empty capsules and b) oil-containing capsules.

experimental set-up (dn/dc = 0.157 ± 0.007). The values obtained were an average of 5–6 measurements.

2.4.3. Optical microscopy (OM)

The prepared capsules were observed, both in dry and wet states, with a Digital Microscope Leica DMS1000. The software ImageJ (version 1.52 publicly available from the National Institutes of Health, Bethesda, MD, USA) was used to measure capsule diameter. The diameter of 20–25 capsules of each batch was measured before calculating the average value and its corresponding sampling error.

2.4.4. Environmental scanning electron microscopy (ESEM)

The outer surface and the cross-section of the dry empty capsules were characterized by ESEM using a FEI Quanta 200 FEG in high vacuum mode, using a secondary electron detector and an accelerating voltage of 20 kV. Before the analysis, the samples were coated on a tape surface with gold by a quorum Q150TS Plus sputter coater. To observe the cross-section, Leica CM 1950 Cryostat was used. The sample was mixed with an embedding medium (OCT Compound) and frozen at −25 °C on an aluminium support inside the machine. Once frozen, the sample was cut and deposited on a microscopic slide.

In the case of oil containing capsules to avoid any sensor contamination due to oil evaporation, observation was carried out at low vacuum and without gold coating.

2.4.5. Thermogravimetric analysis (TGA)

TGA was performed using ALU OXIDE crucibles of 70 µL (ME-24,123) with a Mettler Toledo TGA2 thermobalance. The dynamic test was performed on all the samples weighing around 20 mg between 30 and 800 °C at a heating rate of 10 °C/min in air atmosphere (flow rate of 50 cm^3/min).

2.4.6. Dynamic mechanical analysis (DMA)

DMA was carried out using a DMA Q800 V21.3 Build 96 from TA instruments working on a controlled compression force on the capsule samples. 15 capsules from the different samples were examined.

Temperature, stress, strain, force, and displacement of the capsules were recorded versus time under a ramp force of 2 N/min until rupture occurs. The force vs. displacement graph for each capsule was plotted to determine the corresponding stress at break, assuming all capsules have a spherical shape. Furthermore, the Youngs modulus was calculated using Hertz theory and assuming a Poisson's ratio of 0.5 (Kaygusuz et al., 2016; Chan et al., 2011).

2.4.7. Gas chromatography

To calculate the EE of oil-containing, gas chromatography (GC) was performed by 7890A GC system chromatograph and a 5975C inert MSD with Triple-Axis Detector as a mass detector, both from Agilent Technologies. The test was done after the maturation step on a sample of the crosslinking bath in which the capsules were formed. The method involved extracting non-encapsulated (NE) oil from a coagulation bath sample using hexane through liquid-liquid extraction. The extracted oil was then analyzed using gas chromatography (GC) to determine its quantity based on the area obtained in the analysis. Reference samples with known oil concentrations were prepared to facilitate the calculation of the NE oil quantity in the samples. The encapsulation efficiency (EE) of the oil was calculated according to the following equation:

$$EE = \left(\frac{TO - NE}{TO}\right) * 100 \quad (1)$$

Where TO is the total amount of oil added during the capsule formation

3. Results and discussion

3.1. Alginate characterization

As previously explained, three different batches of sodium alginate were examined in this study. The M/G ratio, which indicates the ratio of the mannuronate blocks to the guluronate bock in the alginate chain, and the molecular weight, are the main characteristics that determine its physical and functional properties (Zha et al., 2024). Indeed, it has been proved before in literature that the variation of the M/G ratio can affect the different structural and mechanical properties of the final gels formed (Zhao et al., 2024). Less rigid, more elastic materials are expected out of alginates with higher M content.

The M/G ratio was determined using the ^{1}H NMR spectroscopy. The spectra of the sodium alginates are shown in Fig. 2 and Figure S1. The characteristic peaks relative to G and M blocks are observed at 5.4–5.6 ppm (I) and at 5.0–5.2 ppm (II), respectively corresponding, the former to the anomeric hydrogen of G unit and the latter to the anomeric hydrogen of M unit and also to H5 of the alternating blocks GM according to the literature (Kinh et al., 2007). The areas of peak I and deconvoluted peak II, are used to calculate the M/G ratio of the corresponding alginate sample, which are shown in Table 2. Alginates A and B exhibit similar ratio, closer to 2, showing that M blocks are predominant over G blocks. Alginate type C, however, shows a ratio of 0.8.

Nevertheless, the final properties of the alginate hydrogels are strongly affected by molecular weight (Wang et al., 2024): indeed, the higher the molecular weight, the higher the number of interactions with the divalent cations to form stronger gels.

The weight average molecular weight (M_w), polydispersity index ($M_{w/}$ M_n), sample fraction with M_w >300 kDa, intrinsic viscosity [η], and hydrodynamic radius (R_h) of the three alginates, calculated by SEC-TDA analysis, are presented in Table 2.

Results indicate different chain length for the tested polymeric samples, with sample B showing the highest and sample C exhibiting the

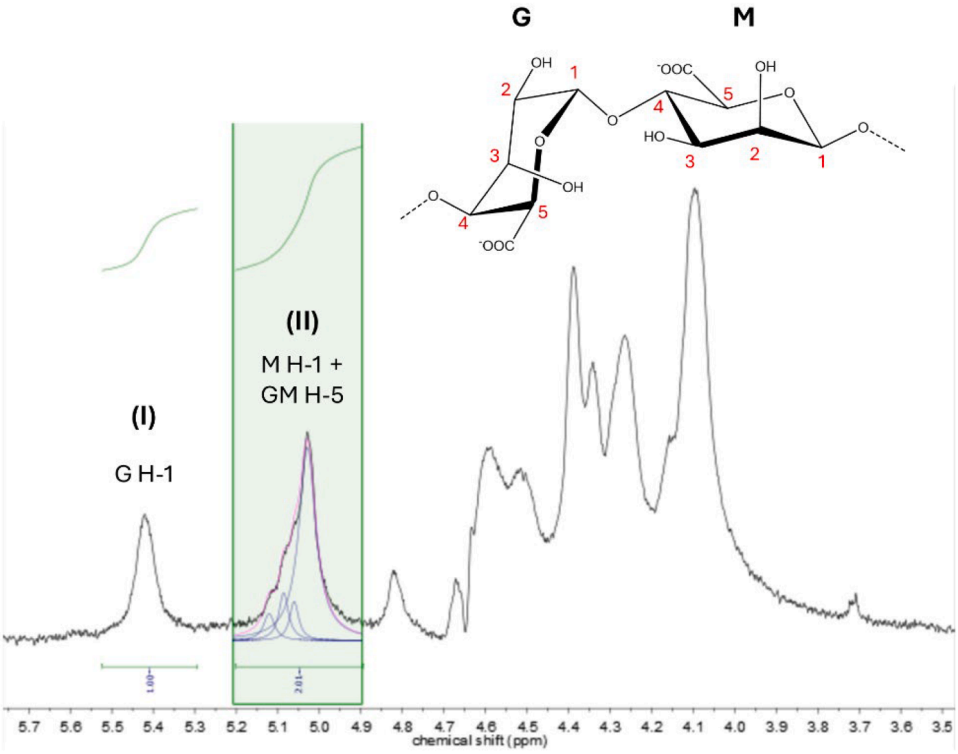

Fig. 2. NMR Spectrum of alginate sample B.

Table 2
Results of the M/G ratio estimation and the SEC-TDA characterization for the alginate samples: weight average molecular weight (Mw), polydispersity (Mw/Mn), sample fraction with M_w >300 kDa, intrinsic viscosity [η], hydrodynamic radius (Rh).

Sample	M/G	M_w (kDa)	M_w/M_n	Sample with M_w >300 kDa (wt%)	[η] (dL/g)	R_h (nm)
A	1.8	230 ± 10	1.2 ± 0.1	24 ± 5	10.4 ± 0.2	32 ± 1
B	1.7	280 ± 20	1.2 ± 0.2	48 ± 5	12.6 ± 0.1	37 ± 1
C	0.8	66 ± 2	1.9 ± 0.1	3± 0	3.2 ± 0.1	13.7± 0.1

lowest M_w value. Sample A shows intermediate chain length with a M_w value close to sample B. However, all the hydrodynamic parameters but polydispersity of sample A are significantly different from sample B) ($p < 0.01$). Sample C shows the broadest molecular weight distribution. The intrinsic viscosity and the hydrodynamic radius values vary consistently with the M_w.

3.2. Capsules preparation and morphological characterization

To optimize the process of capsules preparation, several parameters were studied. The process conditions were first tuned on the preparation of empty capsules crosslinked with zinc chloride, as described in the experimental section. The capsule morphology was studied by OM in parallel with their preparation and it is shown in Fig. 3. The initial trial for capsule preparation used 1 % w/w alginate and 0.5 % w/w zinc chloride (samples A1-Zn0.5 and B1-Zn0.5). However, the capsules formed exhibited a very agglomerated, non-spherical, and flat morphology (Fig. 3-i). This is attributed to the low amount of crosslinker present that is not sufficient to form a stable spherical capsule structure. Indeed, we should keep in mind that the process begins when the outer surface of the alginate drops meets the crosslinker solution and a first, thin wall of alginate precipitates; afterwards, during maturation time more cations move into the drops and determine the growth of the capsule shell. Cation diffusion is driven by the concentration gradient between the inside of the capsules and the crosslinking solution (Pathak et al., 2010). Therefore, the next step was to increase the $ZnCl_2$ concentration to 2 %w/w (samples A1-Zn2 and B1-Zn2), keeping the other parameters unchanged. This led to a less agglomerated, more regular shape due to a denser and more stable structure (Bennacef et al., 2023). However, the capsules were not fully spherical; instead, they looked like half spheres with one flat side. The flat surface is probably formed when the capsules are extruded as drops and they hit the surface of the crosslinking bath; hence, this effect can be reduced by increasing the viscosity of the extruded alginate solution making the drops denser and thus being able to form more spherical capsules (Essifi et al., 2021; Gómez-Mascaraque et al., 2023). This was achieved by increasing the concentration of the alginate solution from 1 to 2 %w/w (sample A2-Zn2) which resulted in the formation of spherical beads. Finally, after optimizing alginate and zinc concentration, the crosslinking bath was changed to calcium chloride, to form reference capsules to which we could check the effect of zinc incorporation. Analogously, capsules prepared in a calcium chloride cross-linking solution (A2-Ca2) had a spherical shape when dried (Fig. 3-v).

Regarding the different alginates, alginates A and B were capable to form capsules, in the previously described conditions. However, using alginate C (Table 1, experiments C1-Ca2 and C2-Ca2) capsules were not formed which can be expected on the basis of its low molecular weight and low viscosity. In this case, the alginate chains do not have enough crosslinking sites and lack the structural integrity to form a stable capsule (Goh et al., 2012). Consequently, alginate type C was discarded for the rest of the experiments. On the other hand, alginate A and B were both used in the capsules' preparation with 1 %w/w alginate and 2 % w/w zinc (samples A1-Zn2 and B1-Zn2) to check whether molecular weight chains affect the capsule's final characteristics.

After optimizing empty capsules' preparation, LO encapsulation was attempted. In order to encapsulate the LO in alginate a nanoemulsion is needed, due to the hydrophobicity of the oil and the hydrophilicity of the alginate solution. In the presence of a surfactant, which is Mowiol 18–88 in this case, LO can be dispersed as tiny droplets in the aqueous phase containing sodium alginate. The oil was broken down into nanosized droplets using an ultraturrax and high-speed homogenization, creating fine suspensions. These suspensions were then extruded into a crosslinker aqueous solution, causing the precipitation of crosslinked alginate on the surface of the oil nanodroplets.

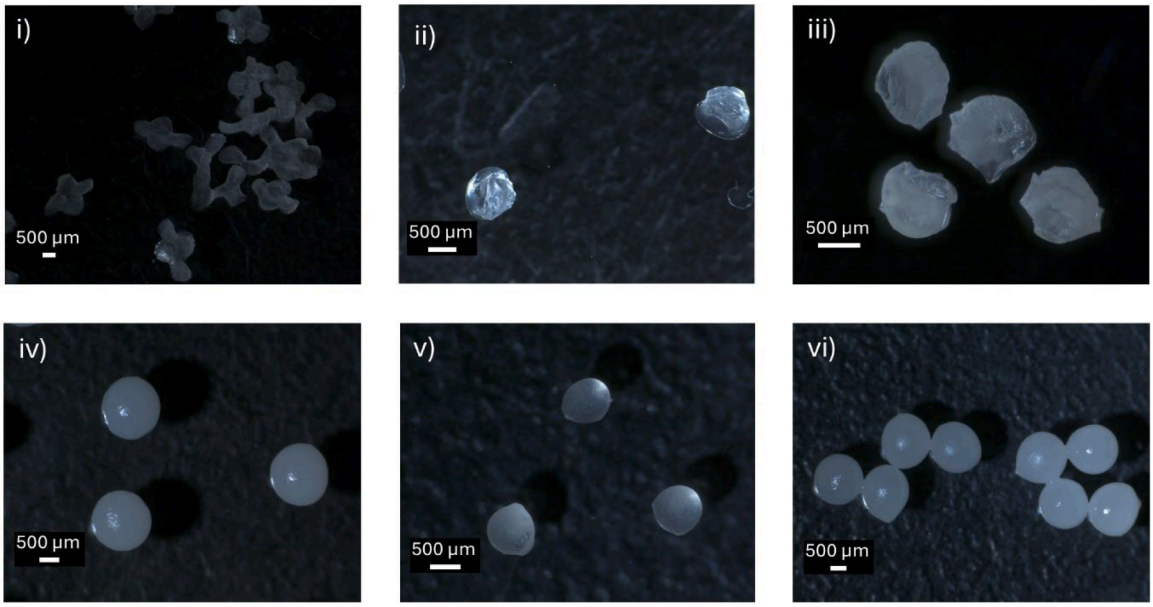

Fig. 3. Optical microscope images of dry capsules of samples i) A1-Zn0.5, ii) A1-Zn2, iii) A2-Zn2, iv) A2-Zn2-O, v) A2-Ca2, and vi) A2-Ca2-O.

Different oil/ alginate ratios were tested. Initially, based on our previous experience, a 1:5 ratio was tested which formed a stable emulsion for at least 19h. To encapsulate more oil, a ratio of 1:3 was also tested. Nevertheless, the formed emulsion resulted unstable: indeed, after 30 mins of homogenization with the ULTRA TURRAX, we could not get uniform o/w dispersions. Therefore, this study was performed using a 1:5 ratio preparation.

By OM, it is notable that not all the capsules have a spherical and uniform shape. The capsules observed after the maturation phase and before drying, whether containing oil or not, present a perfectly spherical and uniform shape due to their water content. However, once dried the capsules present a discrepancy in their morphology.

The values of the diameters of the different capsules calculated using the ImageJ software are reported in Table S1. The average diameter of the wet capsules, which is 2 mm regardless of the composition, is mainly determined by the diameter of the needle used for extrusion (McClements, 2017). The diameters of the empty dry capsules for different compositions are similar, being on average 0.9 mm. The same stands for dry capsules with oil with an average of 1.4 mm. As expected, capsules with encapsulated oil have a slightly larger diameter than empty capsules, and their diameter decreases less during drying. On average, the diameter reduction is 1 for empty capsules and 0.5 for oil-containing capsules. No significant differences were observed based on the type of alginate used.

All these observations were confirmed by ESEM images shown in Fig. 4 and Figure S2. Comparing the samples A2-Zn2 and A2-Ca2 (Fig. 4-a,i and Fig. 4-a,ii), sample A2-Ca2 shows a more spherical and smoother surface while sample A2-Zn2 looks more irregular (Cano-Vicent et al., 2023). Both samples reveal a homogeneous and dense cross-section.

For capsules with oil and formed in a 2 %w/w zinc solution and 2 % w/w alginate (sample A2-Zn2-O), the ESEM images show a much smoother and a perfectly spherical outer surface. These samples show a porous spongy cross-section compared to empty capsules. It is reasonable to conclude that the oil is placed in these pores, in accordance with previous studies where essential oils were encapsulated (Bastos et al., 2020; Soliman et al., 2013). Small, lined holes are observed on the surface of the capsules in sample A2-Zn2-O (Fig. 4-b,iv), which are attributed to residual drops of nanoemulsions remaining during capsule formation. After comparison of the diameters of the inner cavities (~ 0.024 ± 0.005 mm), the small holes on the surface (~ 0.015 ± 0.004 mm) and the diameters of the nanoemulsions studied under the microscope (~ 0.030 ± 0.005 mm) we can confirm this hypothesis, given their close values. The capsules from the sample A2-Ca2-O present the same porous interior with a smooth surface, but there are no lined holes on the surface. This may be because once zinc is coordinatively cross-linked, it becomes more difficult to adjust or modify the interactions it creates compared with calcium.

3.3. Capsules' characterization

3.3.1. Encapsulation efficiency

The results of the encapsulation efficiency as calculated from GC–MS are represented in Table 3 for the different types of capsules. An average of 98 % of the encapsulated oil was retained in all capsules when the crosslinking bath was analyzed directly after the maturation phase. No differences are observed between the different capsule compositions regarding the concentration of either the alginate or the crosslinking ions. This high retention suggests that the nanoemulsion, along with the polymeric barrier, is effective in keeping the oil inside the capsules. However, it is important to note that this value is measured right after the maturation phase, before the drying process; indeed, some oil loss occurs during drying at room temperature. It must be remarked that some evaporation is inevitable due to the oil absorbed on the capsule surface.

3.3.2. Thermogravimetric characterization

A thermogravimetric study in air was conducted to assess the composition of empty capsules, specifically the uronates per cation and the water content. The TGA curves (Figure S3) show that alginate typically exhibits several characteristic weight loss steps. The first weight loss, occurring between 30 °C and 170–200 °C (depending on the crosslinking ion used), is attributed to the water evaporation from the capsules (Kabalan et al., 2023). This demonstrates that the capsules can retain water even after drying, consistent with the hydrophilic nature of alginate. Moreover, for Zn-alginate beads, Extended X-ray Absorption Fine Structure (EXAFS) analysis reveals that water is directly involved in Zn^{2+} coordination sphere (Reig-Vano et al., 2023). Subsequent weight loss steps correspond to the decomposition of the organic alginate matrix and the formation of the metal oxide (Zhang et al., 2011; Khoj, 2024).

From TGA curves, the quantity of uronates per cation and the water content can be estimated for the empty capsules (P. Agulhon et al.,

Table 3
The encapsulation efficiency (%) of LO in the different samples.

Sample	A1-Zn2-O	B1-Zn2-O	A2-Zn2-O	A2-Ca2-O
Encapsulation Efficiency (%)	98.3 ± 0.2	98.4 ± 0.1	98.3 ± 0.2	98.1 ± 0.2

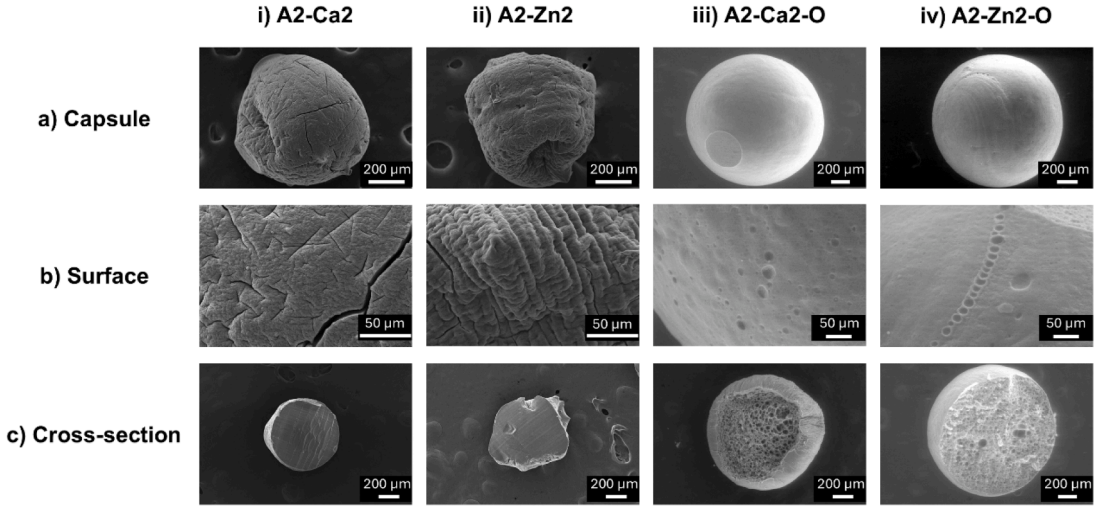

Fig. 4. ESEM photos of the a) capsules, b) surface, and c) cross-section for samples: i) A2-Ca2, ii) A2-Zn2, iii) A2-Ca2-O, and iv) A2-Zn2-O.

Table 4
The uronate/cation ratio and the water/cation ratio of the capsules.

Sample	A1-Zn2	B1-Zn2	A2-Zn2	A2-Ca2
Uronate/cation (mol/mol)	1.99	2.15	2.06	1.03
Water/cation (mol/mol)	1.44	1.62	2.35	2.05

Table 5
Mechanical properties of the different capsules.

Sample	**A2- Zn2**	**A2-Ca2**	**A1-Zn2-O**	**A2-Zn2-O**	**A2-Ca2-O**
Young Modulus E (MPa)	$(2.5 \pm 0.9)*10^3$	$(2.2 \pm 0.6)*10^3$	4.7 ± 1.6	20.3 ± 10.2	46.1 ± 5.6
Stress at break σ_b (MPa)	33.4 ± 16.7	$\sigma_{b>}$ (18/S) [a]	2.2 ± 0.5	3.9 ± 0.6	2.3 ± 0.9
Force at break F_b (N)	8.9±4.0	$F_b > 18$ [a]	2.3±0.2	4.4±0.8	3.9±1.4

S: the cross-sectional surface area of the capsule.
[a] the maximum force of the instrument which is 18 N was not enough to break the sample.

2012); the corresponding results are presented in Table 4. The ratios are around 2 and 1for zinc and calcium, respectively, in agreement with our previous findings (Reig-Vano et al., 2023). This can depend on more complex and often coordinative interactions between alginate and zinc, while calcium tends to establish simple ionic interactions (P. Agulhon et al., 2012).

For the oil-containing capsules, the TGA thermogram differs as expected. After the water evaporation phase, there is a single large weight loss step, which represents both the evaporation of the oil from the capsules and the degradation of alginate. It is observed that the oil in

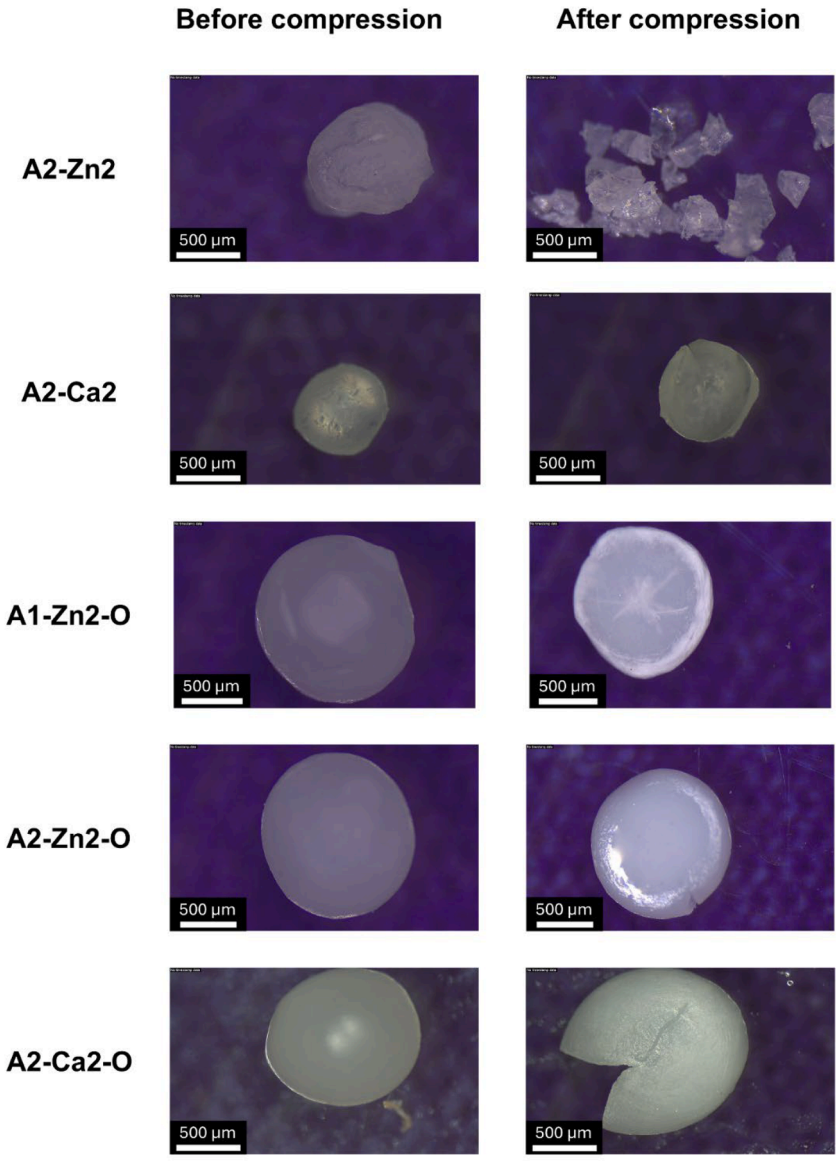

Fig. 5. Images of capsules of samples A2-Zn2, A2-Ca2, A1-Zn2-O, A2-Zn2-O, and A2-Ca2-O before and after the compression test.

zinc-crosslinked capsules starts evaporating faster than in calcium crosslinked capsules.

When comparing the samples A1-Zn2-O and A2-Zn2-O it is evident that the increase in the polymer concentration increases the thermal stability of the capsules and delays the oil evaporation. This is also observed when zinc is replaced by calcium (samples A2-Zn-O and A2-Ca2-O). No major differences are noted between the TGA curves of alginates A and B whether for empty or oily capsules (Figure S3).

In view of the similarity between the two types of alginates studied (A and B) regarding the capsule morphology and composition, it was decided to focus the following studies exclusively on the characterization of the capsules based on alginate A.

3.3.3. *Mechanical characterization*

After the drying phase, the capsules of samples A2-Zn2, A2-Ca2, A1-Zn2-O, A2-Zn2-O, and A2-Ca2-O were mechanically characterized under a compression ramp force of 2 N/min that ranged between 0 and 18 N. The corresponding values of the Young Modulus (E), Stress at break (σ_b) and Force at break (F_b) are reported in Table 5. The images of the studied capsules before and after the compression test are shown in Fig. 5.

Regarding the empty capsules, the capsules made with zinc (sample A2-Zn2) have a slightly higher E compared to those made with calcium, indicating greater rigidity. This is due to the stronger and more directional coordinative bonds formed between zinc and alginate, especially in alginates with a higher M/G ratio (Iskandar et al., 2019). On the other hand, it is also observed that the sample A2-Ca2 did not break under the compression force; however, it shows the formation of very small cracks, while the zinc-crosslinked sample is shattered into pieces (Fig. 5). This indicates that the capsules formed with calcium are stronger and the maximum applied force (18 N) cannot break them. Moreover, the E values of sample A2-Zn2 are more scattered than those of A2-Ca2. This suggests the presence of inhomogeneities in Zn-crosslinked network, probably due to the formation of a more rigid outer wall, which limits cation diffusion (Reig-Vano et al., 2023).

On the other hand, when comparing the oil-containing capsules, samples A1-Zn2-O and A2-Zn2-O, it is shown that the latter has higher values of all the mechanical parameters measured. This aligns with expectations, as a higher amount of alginate in the capsules increases the total crosslinking, resulting in a stronger shell (Kaklamani et al., 2014).

To understand the behavior of the oil-containing capsules, the results can be interpreted as a sum of two factors: the strength of the crosslinking and the plasticizing effect of the oil. Concerning samples A2-Zn2-O and A2-Ca2-O, the Ca-based capsules show a more rigid and fragile structure while the ones with zinc are more ductile and flexible: this is evidenced by higher E and the F_b in Ca-based capsules.

Nevertheless, the optical microscope images of the oil-containing capsules show that, regardless of the cation used, the capsules exhibit elastoplastic behaviour. They first deform elastically under stress, and, once a certain limit is exceeded, they retain permanent deformation even after the stress has been removed (Fig. 5). The capsules flatten under compression and display some cracks.

In view of this microscopic observation, but also of lower E and F_b values of the oil-containing capsules, it is clear that they are more flexible than the empty ones, regardless of the cation used. This can be attributed to their inner porous structure which facilitates crack propagation and capsule rupture (Boccaccini et al., 1997). In fact, this aspect can be advantageous for the topical application of the capsules, where the active principle needs to be released or "squeezed out" through simple manual pressure.

4. Conclusions

The preparation of LO-containing alginate capsules crosslinked with zinc was successfully achieved by a fast and easy procedure, based on the combination of nanoemulsion and ionic gelation, getting an average encapsulation efficiency of 98 %. Ca-containing capsules were also prepared as a reference system. The study was performed by preparing both empty and oil-containing capsules with different proportions of cations and alginate, followed by their characterization in terms of composition, morphology, thermal stability and mechanical properties.

The uronate/cation ratio results 2 for zinc-based capsules due to its coordinative crosslinking, whereas the calcium-based samples have a ratio of 1 due to their predominantly ionic crosslinking. Interestingly, TGA showed that oil-containing capsules crosslinked with calcium can retain and protect LO more than zinc-based ones.

Capsules prepared with 2 % alginate and 2 % zinc or calcium are the most spherical -shaped and dense ones, while those containing oil have highly porous interior as a consequence of oil encapsulation. This composition has been finally selected to test its possible application in acne treatment. Regarding mechanical characterization, calcium-based empty capsules are stronger than zinc-based ones. Capsules LO-containing show similar properties regardless of the cation used, with significantly greater ductility and flexibility compared to the empty capsules, which could be advantageous for their application.

Summing up, in view of the results obtained, there is potential for the application of these beads in acne treatment. Therefore, to deepen this aspect, in a forthcoming paper the study of LO stability and release, as well as the antibacterial activity of the capsules and the possible synergistic effect between LO and zinc, is reported.

CRediT authorship contribution statement

Yasmin Kabalan: Writing – original draft, Methodology, Investigation, Formal analysis. **Héloïse Bernarda:** Writing – original draft, Methodology, Investigation, Formal analysis. **Xavier Montané:** Writing – review & editing, Validation, Supervision, Resources, Project administration, Funding acquisition, Formal analysis, Data curation, Conceptualization. **Silvia De la Flor:** Methodology, Investigation, Formal analysis. **Bartosz Tylkowski:** Validation, Supervision, Resources, Project administration, Funding acquisition, Formal analysis, Data curation, Conceptualization. **Anna Trojanowska:** Methodology, Investigation, Formal analysis. **Annalisa La Gatta:** Methodology, Investigation, Formal analysis. **Marta Giamberini:** Writing – review & editing, Validation, Supervision, Resources, Project administration, Funding acquisition, Formal analysis, Data curation, Conceptualization.

Declaration of competing interest

The authors declare that they have no known competing financial interests or personal relationships that could have appeared to influence the work reported in this paper.

Acknowledgments

The authors thank *Universitat Rovira i Virgili* (URV) for financial support of Yasmin Kabalan's pre-doctoral contract (2021PMF-PIPF-24) within its *Marti i Franquès* programme. The authors also thank the Erasmus+ studies program for supporting Ms. Bernarda's stay at URV.

The authors acknowledge Dr. Rita Marimón Picó, Dr. Mariana Stefanova Stankova, Mercè Moncusí Mercadé and Núria Argany Figueras for their help in ESEM analysis (Scientific & Technical Resources Service, Universitat Rovira i Virgili). The authors also acknowledge Generalitat de Catalunya, Agència de Gestió d'Ajuts Universitaris i de Recerca (2021 SGR 00033).

Supplementary materials

Supplementary material associated with this article can be found, in the online version, at doi:10.1016/j.carpta.2025.100766.

Data availability

Data will be made available on request.

References

Agulhon, P., Robitzer, M., David, L., & Quignard, F. (2012a). Structural regime identification in ionotropic alginate gels: Influence of the cation nature and alginate structure. *Biomacromolecules, 13*, 215–220. https://doi.org/10.1021/bm201477g

Agulhon, P., Markova, V., Robitzer, M., Quignard, F., & Mineva, T. (2012b). Structure of alginate gels: Interaction of diuronate units with divalent cations from density functional calculations. *Biomacromolecules, 13*, 1899–1907. https://doi.org/10.1021/bm300420z

Ali, A. S., Nazar, M. E., Mustafa, R. M., Hussein, S., Qurbani, K., & Ahmed, S. K. (2024). Impact of heavy metals on breast cancer (Review). *World. Acad. Sci. J., 6*. https://doi.org/10.3892/wasj.2023.219

Altun, M., Yildirim, N., & Yapici, B. M. (2023). Chemical characterization, antibacterial, antioxidant, and cytotoxic activity of some essential oils against strains causing acne. *Journal of cosmetic science, 74*, 14–30.

Asnaashari, S., Kazemnezhad, M., Masoud, F., & Javadzadeh, Y. (2023). An overview on the anti-acne properties of herbal essential oils. *Journal of herbal medicine, 38*, Article 100642. https://doi.org/10.1016/j.hermed.2023.100642

Bastos, L. P. H., dos Santos, C. H. C., de Carvalho, M. G., & Garcia-Rojas, E. E. (2020). Encapsulation of the black pepper (Piper nigrum L.) essential oil by lactoferrin-sodium alginate complex coacervates: Structural characterization and simulated gastrointestinal conditions. *Food. Chem., 316*, 26345. https://doi.org/10.1016/j.foodchem.2020.126345

Bennacef, C., Desobry, S., Jasniewski, J., Leclerc, S., Probst, L., & Desobry-Banon, S. (2023). Influence of alginate properties and calcium chloride concentration on alginate bead reticulation and size: A phenomenological approach. *Polymers, 15*, 4163. https://doi.org/10.3390/polym15204163

Boccaccini, A. R., Fan, Z., Boccaccini, A., & Fanb, Z. (1997). A new approach for the Young's modulus-porosity correlation of ceramic materials. *Ceramics international, 23*, 239–245. https://doi.org/10.1016/S0272-8842(96)00033

Cano-Vicent, A., Tuñón-Molina, A., Bakshi, H., Sabater i Serra, R., Alfagih, I. M., Tambuwala, M. M., & Serrano-Aroca, Á. (2023). Biocompatible alginate film crosslinked with Ca2+ and Zn2+ possesses antibacterial, antiviral, and anticancer activities. *ACS omega, 8*, 24396–24405. https://doi.org/10.1021/acsomega.3c01935

Casanova, F., & Santos, L. (2016). Encapsulation of cosmetic active ingredients for topical application-a review. *Journal of microencapsulation, 33*, 1–17. https://doi.org/10.3109/02652048.2015.1115900

Cervantes, J., Eber, A. E., Perper, M., Nascimento, V. M., Nouri, K., & Keri, J. E. (2018). The role of zinc in the treatment of acne: A review of the literature. *Dermatologic therapy, 31*, 12576. https://doi.org/10.1111/dth.12576

Chan, E. S., Lim, T. K., Voo, W. P., Pogaku, R., Tey, B. T., & Zhang, Z. (2011). Effect of formulation of alginate beads on their mechanical behavior and stiffness. *Particuology, 9*, 228–234. https://doi.org/10.1016/j.partic.2010.12.002

Chu, C. C., Chew, S. C., & Nyam, K. L. (2021). Recent advances in encapsulation technologies of kenaf (Hibiscus cannabinus) leaves and seeds for cosmeceutical application. *Food Bioprod. Process., 127*, 99–113. https://doi.org/10.1016/j.fbp.2021.02.009

Cimino, C., Maurel, O. M., Musumeci, T., Bonaccorso, A., Drago, F., Souto, E. M. B., Pignatello, R., & Carbone, C. (2021). Essential oils: Pharmaceutical applications and encapsulation strategies into lipid-based delivery systems. *Pharmaceutics, 13*, 327. https://doi.org/10.3390/pharmaceutics13030327

Collier, C. N., Harper, J. C., Cantrell, W. C., Wang, W., Foster, K. W., & Elewski, B. E. (2008). The prevalence of acne in adults 20 years and older. *Journal of the American Academy of Dermatology, 58*, 56–59. https://doi.org/10.1016/j.jaad.2007.06.045

Del Rosso, J. Q., & Kim, G. (2009). Optimizing use of oral antibiotics in Acne Vulgaris. *Dermatologic clinics, 27*, 33–42. https://doi.org/10.1016/j.det.2008.07.006

Dhamecha, D., Movsas, R., Sano, U., & Menon, J. U. (2019). Applications of alginate microspheres in therapeutics delivery and cell culture: Past, present and future. *International journal of pharmaceutics, 569*, Article 118627. https://doi.org/10.1016/j.ijpharm.2019.118627

Essifi, K., Brahmi, M., Berraaouan, D., Ed-Daoui, A., El Bachiri, A., Fauconnier, M. L., & Tahani, A. (2021). Influence of sodium alginate concentration on microcapsules properties foreseeing the protection and controlled release of bioactive substances. *Journal of chemistry, 2021*. https://doi.org/10.1155/2021/5531479

Gatta, A. La, De Rosa, M., Marzaioli, I., Busico, T., & Schiraldi, C. (2010). A complete hyaluronan hydrodynamic characterization using a size exclusion chromatography-triple detector array system during in vitro enzymatic degradation. *Analytical biochemistry, 404*, 21–29. https://doi.org/10.1016/j.ab.2010.04.014

Goh, C. H., Heng, P. W. S., & Chan, L. W. (2012). Alginates as a useful natural polymer for microencapsulation and therapeutic applications. *Carbohydrate polymers, 88*, 1–12. https://doi.org/10.1016/j.carbpol.2011.11.012

Gómez-Mascaraque, L. G., Chambon, V., Trifkovic, K., & Brodkorb, A. (2023). Alginate microcapsules produced by external gelation in milk with application in dairy products. *Food Structure, 37*, Article 100339. https://doi.org/10.1016/j.foostr.2023.100339

Iskandar, L., Rojo, L., Di Silvio, L., & Deb, S. (2019). The effect of chelation of sodium alginate with osteogenic ions, calcium, zinc, and strontium. *Journal of biomaterials applications, 34*, 573–584. https://doi.org/10.1177/0885328219861904

Kabalan, Y., Montané, X., Tylkowski, B., De la Flor, S., & Giamberini, M. (2023). Design and assembly of biodegradable capsules based on alginate hydrogel composite for the encapsulation of blue dye. *International journal of biological macromolecules, 233*, Article 123530. https://doi.org/10.1016/j.ijbiomac.2023.123530

Kaklamani, G., Cheneler, D., Grover, L. M., Adams, M. J., & Bowen, J. (2014). Mechanical properties of alginate hydrogels manufactured using external gelation. *Journal of the mechanical behavior of biomedical materials, 36*, 135–142. https://doi.org/10.1016/j.jmbbm.2014.04.013

Kaygusuz, H., Evingür, G. A., Pekcan, Ö., von Klitzing, R., & Erim, F. B. (2016). Surfactant and metal ion effects on the mechanical properties of alginate hydrogels. *International journal of biological macromolecules, 92*, 220–224. https://doi.org/10.1016/j.ijbiomac.2016.07.004

Khoj, M. A. (2024). Fabrication of silica/calcium alginate nanocomposite based on rice husk ash for efficient adsorption of phenol from water. *RSC advances, 14*, 24322–24334. https://doi.org/10.1039/d4ra04070h

Kinh, C. D., Vinh Thien, T., Thai Hoa, T., & Khieu, D. Q. (2007). Interpretation of 1 H-nmr spectrum of alginate by 1 H-1 H tocsy and cosy spectrum. *Journal of chemistry, 45*, 772–775. https://doi.org/10.15625/4829

McClements, D. J. (2017). Designing biopolymer microgels to encapsulate, protect and deliver bioactive components: Physicochemical aspects. *Adv. Colloid Interface Sci., 240*, 31–59. https://doi.org/10.1016/j.cis.2016.12.005

Monteiro, R. C., & Fernandes, M. (2024). Are antibiotics still relevant in acne? A review of the therapeutic conundrum. *International journal of dermatology, 63*, 306–310. https://doi.org/10.1111/ijd.16854

Pathak, T. S., Yun, J. H., Lee, J., & Paeng, K. J. (2010). Effect of calcium ion (cross-linker) concentration on porosity, surface morphology and thermal behavior of calcium alginates prepared from algae (Undaria pinnatifida). *Carbohydrate polymers, 81*, 633–639. https://doi.org/10.1016/j.carbpol.2010.03.025

Prasad, A. S., Beck, F. W. J., Snell, D. C., & Kucuk, O. (2009). Zinc in cancer prevention. *Nutr. Cancer., 61*, 879–887. https://doi.org/10.1080/01635580903285122

Ramli, R., Malik, A. S., Hani, A. F. M., & Jamil, A. (2012). Acne analysis, grading and computational assessment methods: An overview. *Skin Res. Technol., 18*, 1–14. https://doi.org/10.1111/j.1600-0846.2011.00542.x

Reig-Vano, B., Huck-Iriart, C., de la Flor, S., Trojanowska, A., Tylkowski, B., & Giamberini, M. (2023). Structural and mechanical analysis on mannuronate-rich alginate gels and xerogels beads based on Calcium, Copper and Zinc as crosslinkers. *International journal of biological macromolecules, 246*, Article 125659. https://doi.org/10.1016/j.ijbiomac.2023.125659

Ren, Y., Wang, Q., Xu, W., Yang, M., Guo, W., He, S., & Liu, W. (2024). Alginate-based hydrogels mediated biomedical applications: A review. *International journal of biological macromolecules, 279*, Article 135019. https://doi.org/10.1016/j.ijbiomac.2024.135019

Revenue of the cosmetics industry worldwide 2019-2029, Statista Research Department (2024). https://www.statista.com/forecasts/1272313/worldwide-revenue-cosmetics-market-by-segment (accessed November 18, 2024).

Rostan, E. F., Debuys, H. V., Madey, D. L., & Pinnell, S. R. (2002). Evidence supporting zinc as an important antioxidant for skin. *International journal of dermatology, 41*, 606–611. https://doi.org/10.1046/j.1365-4362.2002.01567.x

Sangsuwan, J., & Sutthasupa, S. (2019). Effect of chitosan and alginate beads incorporated with lavender, clove essential oils, and vanillin against Botrytis cinerea and their application in fresh table grapes packaging system. *Packag. Technol. Sci., 32*, 595–605. https://doi.org/10.1002/pts.2476

Santos, A. C., Morais, F., Simões, A., Pereira, I., Sequeira, J. A. D., Pereira-Silva, M., Veiga, F., & Ribeiro, A. (2019). Nanotechnology for the development of new cosmetic formulations. *Expert Opin. Drug Deliv., 16*, 313–330. https://doi.org/10.1080/17425247.2019.1585426

Searle, T., Ali, F. R., & Al-Niaimi, F. (2022). Zinc in dermatology. *J. Dermatol. Treat., 33*, 2455–2458. https://doi.org/10.1080/09546634.2022.2062282

Selvasudha, N., Goswami, R., Tamil Mani Subi, M., Rajesh, S., Kishore, K., & Vasanthi, H. R. (2023). Seaweeds derived ulvan and alginate polysaccharides encapsulated microbeads–Alternate for plastic microbeads in exfoliating cosmetic products. *Carbohydr. Polym. Technol. Appl., 6*, Article 100342. https://doi.org/10.1016/j.carpta.2023.100342

Siqueira Andrade, S., de S. Faria, A. V., Augusto Sousa, A., da Silva Ferreira, R., Camargo, N. S., Corrêa Rodrigues, M., & Longo, J. P. F. (2024). Hurdles in translating science from lab to market in delivery systems for Cosmetics: An industrial perspective. *Advanced Drug delivery reviews, 205*. https://doi.org/10.1016/j.addr.2023.115156

Soliman, E. A., El-Moghazy, A. Y., Mohy El-Din, M. S., & Massoud, M. A. (2013). Microencapsulation of essential oils within alginate: Formulation and in vitro evaluation of antifungal activity. *J. Encapsulation Adsorpt. Sci., 3*, 48–55. https://doi.org/10.4236/jeas.2013.31006

Sosnik, A. (2014). Alginate particles as platform for drug delivery by the oral route: State-of-the-art. *ISRN pharmaceutics, 2014*, 1–17. https://doi.org/10.1155/2014/926157

Tan, J. K. L., & Bhate, K. (2015). A global perspective on the epidemiology of acne. *The British journal of dermatology, 172*, 3–12. https://doi.org/10.1111/bjd.13462

Vasam, M., Korutla, S., & Bohara, R. A. (2023). Acne vulgaris: A review of the pathophysiology, treatment, and recent nanotechnology based advances. *Biochemistry and biophysics reports, 36*, Article 101578. https://doi.org/10.1016/j.bbrep.2023.101578

Walsh, T. R., Efthimiou, J., & Dréno, B. (2016). Systematic review of antibiotic resistance in acne: An increasing topical and oral threat. *The Lancet Infectious diseases, 16*, 22–32. https://doi.org/10.1016/S1473-3099(15)00527-7

Wang, N., Tian, J., Wang, L., Wen, C., & Song, S. (2024). Polyelectrolyte complex formation of alginate and chito oligosaccharide is influenced by their proportion and alginate molecular weight. *International journal of biological macromolecules, 273*, Article 133173. https://doi.org/10.1016/j.ijbiomac.2024.133173

Wani, S. U. D., Ali, M., Mehdi, S., Masoodi, M. H., Zargar, M. I., & Shakeel, F. (2023). A review on chitosan and alginate-based microcapsules: Mechanism and applications in drug delivery systems. *International journal of biological macromolecules, 248*, Article 125875. https://doi.org/10.1016/j.ijbiomac.2023.125875

Zha, L., Aachmann, F. L., Sletta, H., Arlov, Ø., & Zhou, Q. (2024). Cellulose nanofibrils/alginates double-network composites: Effects of interfibrillar interaction and G/M ratio of alginates on mechanical performance. *Biomacromolecules, 25*, 4797–4808. https://doi.org/10.1021/acs.biomac.4c00093

Zhang, J., Ji, Q., Shen, X., Xia, Y., Tan, L., & Kong, Q. (2011). Pyrolysis products and thermal degradation mechanism of intrinsically flame-retardant calcium alginate fibre. *Polymer degradation and stability, 96*, 936–942. https://doi.org/10.1016/j.polymdegradstab.2011.01.029

Zhang, T., Luo, Y., Wang, M., Chen, F., Liu, J., Meng, K., & Zhao, H. (2020). Double-layered microcapsules significantly improve the long-term effectiveness of essential oil. *Polymers, 12*, 1651. https://doi.org/10.3390/POLYM12081651

Zhao, Z., Zhao, D., Su, L., Ding, M., Zhang, M., He, H., & Li, C. (2024). Encapsulation and release of salidroside in myofibrillar proteinsodium alginate gel: Effects of different M/G ratios of sodium alginate. *International journal of biological macromolecules, 282*, Article 136811. https://doi.org/10.1016/j.ijbiomac.2024.136811